A Multilevel CSI Based Lattice Connected Photovoltaic System

Dilmohan Kumar[#1], Chirag Gupta[*2]

[#] *M.Tech Student&Electrical & Electronics Engineering Department & RKDF University Bhopal, M.P, India*

[*]*Electrical & Electronics Engineering Department & RKDF University Bhopal, M.P, India*

[1]dilmohanikkumar4321@gmail.com

[2] cgupta.011@gmail.com

Abstract *— **This paper proposes a Photovoltaic Grid-connected (PV) device based on the topology of a multilevel Current Source Inverter (CSI). The topology proposed here consists of CSI modules linked in parallel that operate at a very low switching frequency. For the n number of inverter modules, the output results in 2n+1 current level. Each inverter module has its own PV source, Maximum Power Point Tracking (MPPT) unit and DC-link current controller in the multilevel inverter topology. The proposed topology has a single AC-side current controller that limits the requirements for AC-side sensors and filters unlike previously proposed multilevel CSI topologies. Two inverter units were considered in this study to demonstrate the efficiency of the CSI-based multilevel inverter. Simulation studies are performed in the PSCAD/EMTDC environment.***

Keywords *— **Current-Source Inverter (CSI), multilevel, Maximum Power Point Tracking (MPPT), feed-forward, Insolation level.***

I. INTRODUCTION

In recent years, multilevel inverters have gained considerable interest and have been studied for high-voltage and high-power applications. By the number of levels in a given topology, the output voltage in the case of VSI, and the output current in the case of CSI, assuming stair-case waveforms with a greater number of steps compared to single-stage, this results in a near-sinusoidal waveform at a reduced switching frequency with a reduced Total Harmonic Distortion (THD). In addition, multilevel inverter operation at a low switching frequency results in lower switching losses and higher potential for power transfer. In addition, multilevel inverter operation at a low switching frequency results in lower switching losses and higher potential for power transfer.

The multilevel CSI studied in this paper consists of n numbers of connected CSIs capable of generating 2n+1 output current levels in parallel. From its own PV source, each inverter device is energized. The current from each PV array is independently controlled by the DC-link controller, while the AC-side current is controlled by a combined control scheme. The topology used in this paper is able to accommodate PV sources operating at equal and varying levels of insolation. Furthermore, the proposed multilevel CSI-based in terms of filters and sensors, topology is an important system.

II. STRUCTURE OF A TYPICAL PHOTOVOLTAIC (PV) SYSTEM

The main building blocks of a PV system, shown in Figure 1 are described below.

A. PV Array

A PV array consists of a number of PV modules or panels. A PV module is an assembly of a large number of interconnected PV cells.

B. Inverter

In order to transform the DC voltage produced from a PV module to a three-phase AC voltage, the inverter in a PV device is used. Three legs with two switches in each leg have a three-phase inverter. The switching is carried out by Pulse-Width Modulation depending on the carrier or space vector (PWM). Later in this chapter, an extensive discussion on various inverter topologies is given. Usually, the inverter is connected through a transformer to the utility grid. Transformer-less PV inverter topologies for single-phase grid-connected PV inverters have, however, also been suggested and implemented.

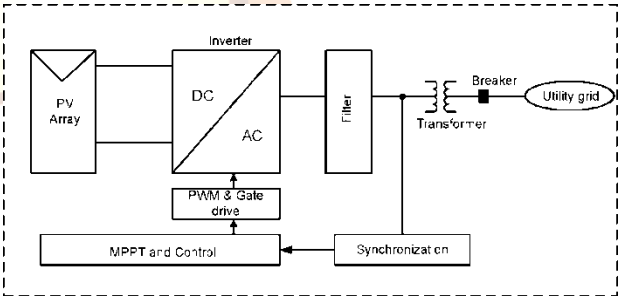

Fig 1 Structure of a typical single-stage PV system

C. Filter

An inverter output quantity (voltage in VSI and current in CSI) is pulsed and includes switching harmonics along with a simple 60 Hz. A filter is necessary at the AC terminal of the inverter, where it is interfaced to the grid, to separate the 60 Hz portion. Because the filter output depends on the impedance of the grid, particular care must be exercised in the filter design.

III. CONTROL STRUCTURE FOR THE PV SYSTEM BASED ON MULTILEVEL CURRENT-SOURCE INVERTER

The DC and AC side currents are required to be controlled by the controller of a grid-connected CSI-based PV system to ensure: (i) a high-quality sinusoidal current is injected into the grid from all inverters, (ii) the actual power injected into the grid is equal to the amount of the maximum power that can be extracted from the PV panel under all conditions, and (iii) the reactive power at the interface with the grid assumes the desired value. As Fig2.illustrated, Pulse Width Modulation (PWM) and CSI control must be synchronized into a Phase Locked Loop (PLL) to the grid voltage. Fig.2 also shows that the error signals between the reference commands i_{sdref1} and i_{sdref2} are processed by two PI controllers, m_d and m_q, from two inverters and i_{sdref}, to produce modulating signals. Although the PI controller is simple in structure and easy to implement, ample insight is needed for proper tuning of its parameters. In this section, an intuitive method is proposed for tuning the PI controller parameters.

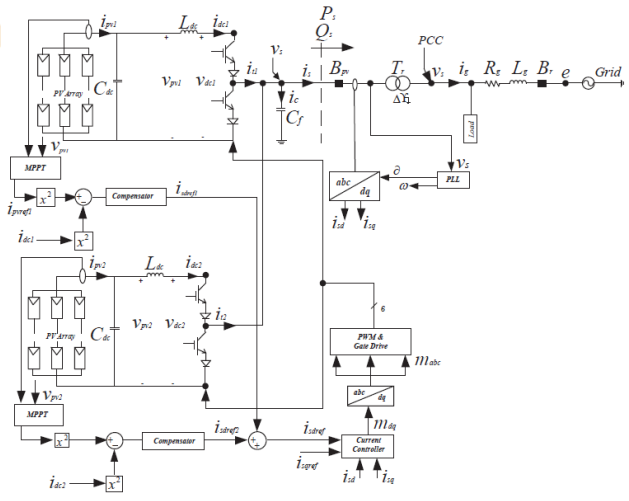

Fig. 2. Single-line schematic diagram of the three-phase, multi-level, grid-connected PV system based on CSI

A. Phase-Locked-Loop (PLL)

The AC variables of the PV system are projected on a d_q unit, which rotates at an angular speed ω, to simplify the control structure. The AC variables are sinusoidal functions of the grid frequency in the steady state, around ω_0. If the angular dq-frame speed is set to the grid frequency, the transformed quantities become steady-state time-invariant, simplifying designing the controller. This is accomplished through a Phase Locked Loop (PLL), the block diagram of which is given in Fig.3.The figure shows that the input to the PLL block is the Typical Coupling Point (PCC) sinusoidal-varying voltage and the output is the abc-to-dq and dq-to-abc transition angle, δ. The voltage is resolved into d- and q-axis based elements. Just in Fig. 3 using a PI controller, the voltage v_{sq} is regulated to zero, H (s). Regulating the q-axis voltage component to zero renders the active and reactive powers, P_s and Q_s, independent of the v_{sq} voltage. Thus, in terms of i_{sd} and i_{sq} currents, active power, P_s and reactive power, Q_s can be expressed as:

$$P_s = \frac{3}{2} v_{sd} i_{sd} \quad (1)$$

P_s is therefore proportional to, and can be regulated by, i_{sd}. Similarly, the term dq-frame for reactive power takes the form of:

$$Q_s = -\frac{3}{2} v_{sd} i_{sd} \quad (2)$$

Equation (2) shows that the i_{sq} can be used to monitor Q_s.

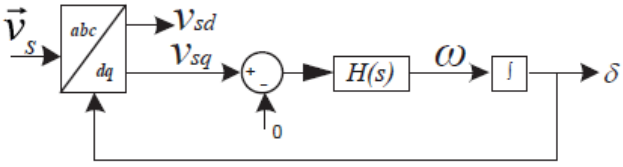

Fig. 3. Block diagram of the Phase-Locked Loop (PLL)

B. Design of Inner Current Control Loop

Equations (1) and (2), respectively, show that it is possible to change the active and reactive powers given by the CSI by regulating i_{sd} and i_{sq}, respectively. Fig. 4 displays the CSI AC-side Current Controller block diagram. $K_d(s)$ and $k_q(s)$ controller structures in Fig.4 are represented as:

$$k_d(s) = k_q(s) = k_p + \frac{k_i}{s} \quad (3)$$

Where the proportional and integral gains, respectively, are k_p and k_i. The m_d and m_q control signals are obtained as

$$m_d = \frac{i_{tdref}}{i_{dc}} \text{ and } m_q = \frac{i_{tqref}}{i_{dc}} \quad (4)$$

Wherei_{tdref} and i_{tqref} are existing references derived from the outputs of the $k_d(s)$ and$k_q(s)$ compensators, respectively. The d-axis part of the output current of the inverter, i_{td}, is associated with the i_{sd} current as:

$$i_{td} = i_{cd} + i_{sd} \tag{5}$$

Where i_{cd} is a d-axis part of the current of the filter capacitor. It should be noted that the basic frequency portion of the capacitor current would be very small with a proper filter design, i.e., i_{cd} is negligible as compared to i_{sd}. For the q-axis elements, the same claim can be made.

Therefore, we can write

$$i_{td} \approx i_{sd} \approx m_d i_{dc} \; and \; i_{tq} \approx i_{sq} \approx m_q i_{dc} \tag{6}$$

The following transfer, under the assumption that $i_{cd} = 0$.

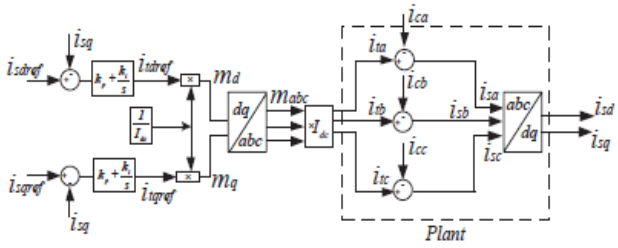

Fig. 4. Block diagram of the CSI AC-side current control system

For the closed-loop control system, function can be writteni_{sq}, shown in Fig. 4.

$$T(s) = \frac{i_{sd}}{i_{sdref}} = \frac{k_p + \frac{K_i}{s}}{k_p + \frac{k_i}{s} + 1} = \frac{s\frac{k_p}{k_p+1} + \frac{k_i}{k_p+1}}{s + \frac{k_i}{k_p+1}} \tag{7}$$

The pole of the transfer function $T(s)$ in (7) approaches the origin of the s-plane as the value of k_p increases, which is not desirable. Therefore, k_p should be selected to be small to imitate the transient behavior of a first order system. $k_i$is chosen in the range of 0.5 ms, as the inverse of time-constant, to 5 ms in order to get a fast and precise response.

k_p and k_i can again be described as:

$$k_p \approx 0 \; and \; k_i = \frac{1}{\tau_i} \tag{8}$$

and substituting the values of k_p and k_i in (7), the transfer function $T(s)$ becomes

$$T(s) = \frac{i_{sd}}{i_{sdref1} + i_{sdref2}} = \frac{\frac{1}{\tau_i}}{s + \frac{1}{\tau_i}} = \frac{1}{\tau_i s + 1} \tag{9}$$

C. *Design of Outer Current Control Loop*

Since the outer current control structures of the two inverters are identical, the following sections explain the detailed control structure of the top inverter.

The CSI of outer controller is designed based on the equation:

$$\frac{1}{2} L_{dc} \frac{di_{dc1}^2}{dt} = P_{pv1} - \frac{3}{2}\left(v_{sd} i_{sd} + v_{sq} i_{sq}\right) \tag{10}$$

Where the power provided by the PV array is P_{pv}. After substituting $v_{sq} = 0$, Equation (10) represents a device with i_{sd} as the input, i_{dc}^2 the output is dc and the disturbance input is v_{sd}. If the time constant τ_i is correctly selected in the current controller's PI compensator, i_{sd} can be approximated to i_{sdref}. Therefore (10) can, be rewritten as:

$$\frac{1}{2} L_{dc} \frac{di_{dc1}^2}{dt} \approx P_{pv1} - \frac{3}{2}\left(v_{sd} i_{sdref1}\right) \tag{11}$$

The current controller of a DC-link constructed on the basis of (11) is shown in Fig. 5. According to 11, the fact that $v_{vp}$and i_{dc} are a result of P_{pv} renders the device nonlinear. i_{sdref}can be derived in the following manner to minimize the effect of nonlinearity:

$$i_{sdref} = u_i + \eta \underbrace{\left(\frac{P_{pv1}}{\frac{3}{2} v_{sd}}\right)}_{i_{ff1}} \tag{12}$$

Where u_i is a new input for the control, shown in Fig. 5, and i_{ff} is a feed-forward signal that can be allowed or disabled when the value unit or zero is assumed by the binary multiplierη. Substituting (12) in (11) for i_{sdref}, we gets

$$\frac{L_{dc}}{2} \frac{di_{dc1}^2}{dt} \approx (1 - \eta) P_{pv1} - \frac{3}{2} v_{sd} u_i \tag{13}$$

Equation (13) indicates that the influence of the nonlinearity of the PV array on the DC-side current control is eliminated if η = 1, and the efficient control unit becomes an integrator.

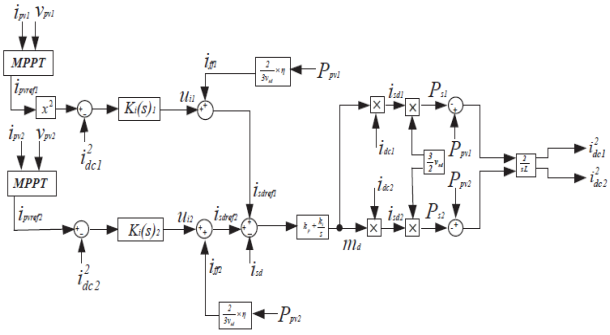

Fig. 5. Control Structure of multilevel CSI-based PV system

IV. SIMULATION RESULTS

Fig. 6 due to a massive step change in insolation stage presents the response of the PV system based on multilevel CSI. The simulation takes place in the framework of PSCAD/EMTDC. The degree of insolation at t = 1s ranges from 0.8 kW/m^2 to 1 kW/m^2, as shown in Fig.6(a). Current references from the MPPTs increase due to changes in insolation level, which in turn raises the multilevel CSI terminal current, as illustrated in Fig. 6(b). With the shift in MPPT reference values, the output from the DC-link controller increases, causing the current injected into the grid to change, as shown in Fig. 6(c). The current i_{sdq} is the component of the d-axis and q-axis of the current i_s.The q-axis part of the current i_s is controlled to zero by the AC-side current controller in order to maintain the unit power factor at the Common Coupling (PCC) stage, as shown in Fig. 6(c). Fig. 6(d) demonstrates that the PCC retains a clean sinusoidal current resulting from the multilevel inverter-based PV system and unit power factor.

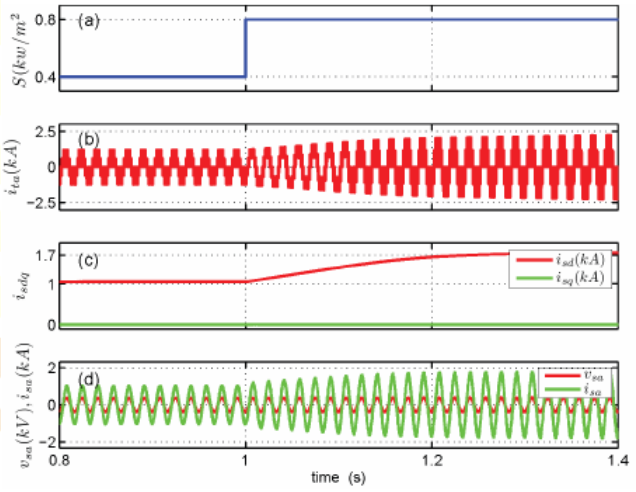

Fig. 6. Response of the PV system to a step change in insolation level (a)Insolation level; (b)Multilevel current at the terminal of the multilevel inverter; (c) *d*- and *q*-axis currents injected into the grid; (d) Voltage and current the Point of Common Coupling (PCC)

V. CONCLUSION

The paper addressed the power circuit and control system architecture for a three-phase, grid-connected PV device multilevel inverter system. In terms of control structure and use of separate DC current sources, the proposed systems vary from those proposed earlier. There are separate MPPT and DC-link controllers in each inverter unit. Independent operation of PV units allows PV units to be accommodated under varying degrees of insolation. A feed-forward control approach is used by the DC-link current controller. The generation of reference signals for the AC-side current controller is contributed by any DC-link current controller. Simulation results for PV systems working under equal levels of insolation were presented in this paper. A combined current control in a dq-frame is applied on the AC side of the inverter. The current controller ensures that the unit power factor of the PV device is operational. In addition, At a low switching frequency and with an inexpensive capacitive filter common to all modules, high quality waveforms are produced. Furthermore, the proposed structure prevents the use of individual current sensors at all modules' AC outputs.

REFERENCES

[1] R. Singh, G. F. Alapatt, and K. F. Poole, "Photovoltaics: Emerging role as a dominant electricity generation technology in the 21st century," in International Conference on Microelectronics, 2012, pp. 53-63.

[2] H. Kim and K. Kim, "Filter design for grid-connected PV inverters," in International conference on Sustaianble Energy Technologies,2008.

[3] H. Patel and V. Agarwal, "A single-stage, single-phase, transformer-less doubly grounded grid-connected pv interface," IEEE Transaction on Energy Conversion, vol. 24, no. 1, pp. 93{101, 2009.

[4] S. Kjaer, J. K. Pedersen, and Blaabjerg, "A review of single-phase grid-connected inverters for Photovoltaic modules," IEEE Transaction on Industry Application,vol. 41, no. 5,

[5] Z. Bai, Z. Zhang, and Y. Zhang, "A generalized three-phase multilevel current source inverter with carrier-phase-shifted spwm," in Power Electronic Specialist Conference, 2007

[6] J. S. S. Prasad and B. G. Fernandes, "Active commutated thyristor csi for grid connected PV application," in International Power Electronics and Motion Control Conference, vol. 3, 2004.

[7] C. Photong, C. Klumpner, and P. Wheeler, "A current source inverter with series connected AC capacitors for photovoltaic application with grid fault ride through capability," in Industrial Electronics Conference, 2007,

[8] D. Z. Zmood and D. G. Holmes, "Improved voltage regulation for current-source inverter," IEEE Transaction on Industry Application, vol. 37, no. 4, pp. 1028-1036, 2001.

[9] R. Badin, Y. Huang, F. Peng, and H. Kim, "Grid interconnected Z-source PV system," in Power Electronic Specialist Conference, 2007.

[10] F. Z. Peng, "Z-source inverter," IEEE Transaction on Industry Application, vol. 39.

[11] W. Hongbin and T. Xiaofeng, "Three-phase photovoltaic grid connected generation technology with MPPT function and voltage control," in International Conference on Power Electronics and Drive System, 2009, pp. 1295-1300.